

Plant embryogenesis requires AUX/LAX-mediated auxin influx

Hélène S. Robert^{1,2*}, Wim Grunewald^{1*}, Michael Sauer^{3,4}, Bernard Cannoot¹, Mercedes Soriano⁵, Ranjan Swarup⁶, Dolf Weijers⁷, Malcolm Bennett⁶, Kim Boutilier⁷ and Jiří Friml^{1,2,8}

¹*Department of Plant Systems Biology, Flanders Institute for Biotechnology (VIB) and Department of Plant Biotechnology and Bioinformatics, Ghent University, 9052 Gent, Belgium;*

²*Mendel Centre for Genomics and Proteomics of Plants Systems, CEITEC MU - Central European Institute of Technology, Masaryk University, 625 00 Brno, Czech Republic;*

³*University of Potsdam, Institute of Biochemistry and Biology, D-14476 Potsdam, Germany;*

⁴*Departamento Molecular de Plantas, Centro Nacional de Biotecnología, Consejo Superior de Investigaciones Científicas, 28049 Madrid, Spain;*

⁵*Wageningen University and Research Centre, P.O. Box 619, 6700 AP Wageningen, The Netherlands;*

⁶*School of Biosciences and Centre for Plant Integrative Biology, University of Nottingham, LE12 5RD Nottingham, United Kingdom;*

⁷*Laboratory of Biochemistry, Wageningen University, 6703 HA Wageningen, The Netherlands;*

⁸*Institute of Science and Technology Austria (IST Austria), 3400 Klosterneuburg, Austria.*

* These two authors contributed equally to this work.

Corresponding author: Friml, J. (jiri.friml@ist.ac.at)

Running title: Auxin influx for embryogenesis

ABSTRACT

The plant hormone auxin and its directional transport are known to play a crucial role in defining the embryonic axis and subsequent development of the body plan. Although the role of the PIN auxin efflux transporters has been clearly assigned during embryonic shoot and root specification, the role of the auxin influx carriers, AUX1 and AUX1-LIKE (LAX) proteins, is not well established so far. Here we used chemical and genetic tools on *Brassica napus* microspore-derived embryos and *Arabidopsis thaliana* zygotic embryos, and demonstrate that AUX1, LAX1 and LAX2 are required for both shoot and root pole formation, in concert with the PIN efflux carriers. Furthermore, we uncovered a positive feedback loop between MONOPTEROS/ARF5-dependent auxin signalling and auxin transport. This MONOPTEROS-dependent transcriptional regulation of auxin influx (AUX1, LAX1 and LAX2) and auxin efflux (PIN1 and PIN4) carriers by MONOPTEROS helps to maintain proper auxin transport to the root tip. These results indicate that auxin-dependent cell specification during embryo development requires balanced auxin transport involving both influx and efflux mechanisms, and that this transport is maintained by a positive transcriptional feedback on auxin signalling.

Key words (>3):

Arabidopsis thaliana embryogenesis, Auxin transport, AUX1 and AUX1-LIKE, MONOPTEROS/ARF5, PIN, *Brassica napus*, microspore

INTRODUCTION

Sexually reproductive organisms develop from a single-cell zygote, the product of fertilization. Divisions of the zygote are precisely controlled in animals and plants and give rise to a population of cells that forms the embryo. In plants, embryos will develop a body plan along a shoot-root axis, containing one or two cotyledons, a shoot apical meristem, a hypocotyl and a root apical meristem. Notably activation of transcriptional signalling pathways of the plant hormone auxin is pivotal for cellular patterning during embryogenesis (Rademacher et al., 2012; Schlereth et al., 2010; Weijers et al., 2006; Yoshida et al., 2014). However, auxins are not synthesized in all cells (Ljung et al., 2005; Petersson et al., 2009; Robert et al., 2013) and are therefore transported from source to sink tissues by specific influx and efflux proteins (Petrásek and Friml, 2009). So far, it is assumed that the plasma membrane-localised PIN efflux proteins are responsible and rate-limiting for the directional auxin flow during embryogenesis (Friml et al., 2003; Weijers et al., 2006). Besides genetic and pharmacological evidence, this hypothesis is supported by the observation that auxin controls the direction of its own transport by regulating both the expression and localisation of the PIN efflux transporters (Sauer et al., 2006a; Vieten et al., 2005). Recently, spatially and temporally defined foci of auxin production during embryogenesis were discovered to feed back on PIN proteins to regulate their polar localization towards sink tissues, where auxin signalling triggers specific developmental programs (Robert et al., 2013; Wabnik et al., 2013). Also, indole-3-acetic acid (IAA), the major form of auxin, passively diffuses into the cytosol in its protonated form, suggesting that auxin efflux is the major mechanism for active auxin transport. However, in specific developmental situations, for example during root gravitropic responses (Swarup et al., 2001), lateral organ initiation and outgrowth (Kierzkowski et al., 2013; Swarup et al., 2008), and root hair development (Jones et al., 2009), passive auxin uptake needs to be supported by the amino acid permease-like proteins of the AUX1/AUX1-LIKE (LAX) family (Bennett et al., 1996; Péret et al., 2012). A detailed analysis of these proteins during early embryogenesis has not been reported. So far it was only demonstrated that members of the AUX1/LAX family are redundantly required for correct cell organisation in the radicle tip of mature embryos (Ugartechea-Chirino et al., 2009). Here, we show that AUX1/LAX dependent-auxin influx is needed for cellular patterning from early embryogenesis onward and that the expression of *AUX1* and *LAX2* is controlled by the MP-BDL signalling pathway. We put forward a model in which auxin influx and efflux systems collaborate to regulate cell specification.

RESULTS

Microspore-derived embryos as tool to study plant embryogenesis in high throughput

The study of molecular processes during plant embryogenesis is often limited by the relatively low sample numbers typically associated with laborious and technically challenging preparation methods. To overcome this limitation, we tested the potential of microspore-derived *in vitro* embryos of *Brassica napus* as an experimental system. Using heat-shock treatments together with specifically adjusted media, microspores isolated from early stage *B. napus* flowers can be induced to develop into suspensor-like structures, mimicking zygotic embryos (Fig. S1; Joosen et al., 2007; Supena et al., 2008). To test whether the microspore-derived *Brassica* embryos would respond in a similar way as zygotic *Arabidopsis* embryos, the effect of a collection of known chemicals on embryo development was investigated. The list consisted of the synthetic auxin analogues NAA and 2,4-D, the auxin antagonist PEO-IAA (Hayashi et al., 2008), the cytokinin BA, auxin transport inhibitors NPA and NOA, and chemicals affecting intracellular protein trafficking (brefeldin A (BFA), tyrphostin A23, wortmannin).

The majority of the microspores cultivated in the presence of 0.1 μM 2,4-D developed into embryos with cotyledon and root pole specification problems (68/82, Fig. S2B). In presence of 1 μM 2,4-D there was an increase in the number of ball-shaped embryos (26/62, Fig. S2C). Incubation of developing embryos in 0.1 or 1 μM NAA did not lead to obvious developmental defects, except for a mild increase in the number of ball-shaped embryos (5/67 and 6/71, respectively compared to 3/154 for DMSO control, Fig. S2L). In line with the reported role of auxin during *Arabidopsis* zygotic embryogenesis (Friml et al., 2003), treatments with the auxin-antagonist PEO-IAA completely blocked *Brassica* microspore embryogenesis, even at low concentrations (Fig. S2K). The same could be observed by adding wortmannin (a strong inhibitor of intracellular protein trafficking) to the developing embryo cultures (data not shown). Also tyrphostin A23 (an inhibitor of endocytosis) strongly affected microspore embryogenesis (Fig. S2L).

Blocking auxin transport by treating the *Brassica* microspore embryos with the auxin efflux inhibitor NPA induced severe patterning defects. At low concentrations (1 μM) NPA interfered with cotyledon initiation and development (31/62), while at higher concentrations (10 μM) it additionally affected apical-basal axis establishment, as demonstrated by the formation of ball-shaped embryos (12/55, Fig. S2G,H). Very similar results were obtained with BFA (Fig. S2D,F), a fungal toxin which affects intracellular trafficking of the PIN auxin

transporters (Geldner et al., 2001). Interestingly, the 2,4-D-, NPA- and BFA-induced phenotypes resembled those observed in *Arabidopsis* auxin transport mutants or upon applying the same compounds to *Arabidopsis in vitro* ovule cultures (Friml et al., 2003). Also for the cytokinin BA, which was previously shown to enhance degradation of the PIN transporters during *Arabidopsis* lateral root initiation (Marhavy et al., 2011; Marhavy et al., 2014), and to repress *PIN* expression in the *Arabidopsis* main root meristem (Růzicka et al., 2009), developmental defects were observed that can be related to a deficient auxin transport system. Incubation of developing microspores in 1 μ M BA induced the formation of triangular shaped embryos with a strong similarity to the 2,4-D treated embryos (Fig. S2I). Thus, these observations show that *Brassica napus* microspore-derived embryos responded to the tested compounds in a very similar way as *Arabidopsis* zygotic embryos and suggest that the auxin transport controlling mechanisms that are intensively studied in *Arabidopsis* are conserved in *Brassica napus*.

Pharmacologic and genetic inhibition of auxin influx affects plant embryogenesis

Of all the compounds tested, the results obtained with the auxin influx inhibitor 1-naphthoxyacetic acid (1-NOA; Parry et al., 2001) were not anticipated, as a role for auxin import during early embryogenesis has not been reported. After adding 1-NOA to microspore embryo cultures, an enhanced frequency of embryos with cotyledon specification and/or root specification problems was observed (60/153, compared to 21/186 for DMSO control, Figs 1A-C, S3). Since it was shown that 1-NOA also partially reduces the activity of auxin efflux carriers (Lanková et al., 2010), we performed a NAA complementation treatment. Uptake of the synthetic auxin NAA is independent of the auxin influx carriers (Delbarre et al., 1996) and should therefore be able to rescue the auxin influx inhibitor related defects. Interestingly, the 1-NOA/NAA double treatment did not influence the root specification problems, but rather reduced the frequency of embryos of small size or with fused cotyledons (4/88 for NOA/NAA treatment compared to 23/153 for NOA alone, Fig. S3). Alternatively, we used 2-NOA which was shown to inhibit auxin import more specifically (Lanková et al., 2010) and found that 2-NOA mainly affected cotyledon development (26/119, Fig. S3). Similar experiments were performed in *Arabidopsis* ovules cultured on 2-NOA for 3 and 5 days. In contrast to *Brassica* microspore embryos, for which treatment started after microspore induction, *Arabidopsis* ovules were cultured starting from later embryonic stages, about three to four days after pollination where the majority of the embryos were at the early globular stage. *Arabidopsis*

ovules treated with 2-NOA produced embryos with weak cotyledon and root phenotypes (7/25 = 28% for 3-day and 25/60 = 41.7% for 5-day treatment, compared to 1/33 = 3.0% and 5/47 = 10.6%, respectively, in DMSO control, Fig. 1G-I). The defects resembled those of *Brassica* microspore embryos cultured in the presence of NOA, i.e. smaller or fused cotyledons or aberrations at the root pole. In these embryos, the expression of the *DR5* auxin response marker (Friml et al., 2003; Ulmasov et al., 1997) was enhanced and more diffuse, compared to DMSO-treated embryos (Fig. 1J-L), possibly because disturbance of auxin influx by application of 2-NOA in post-globular embryos, where the auxin response maximum is already established in the future root pole (Friml et al., 2003; Wabnik et al., 2013), may lead to a more diffuse auxin distribution (Bainbridge et al., 2008).

Taken together, these experiments show that pharmacological inhibition of auxin influx in *Brassica* micropore embryos and zygotic *Arabidopsis* embryos affects cotyledon development. Moreover the defects in root development after NOA treatment, which were not rescued by NAA co-treatment, seemed indirectly linked to auxin influx defects, and appeared to be a consequence of perturbed auxin distribution that affected auxin signalling. These data identify a novel role for auxin import in embryo patterning during plant embryogenesis, probably by ensuring a proper distribution of embryonic auxin.

AUX1, LAX1 and LAX2 are redundantly required for Arabidopsis embryo development

To study the putative role of auxin import during embryogenesis in more detail, we first determined which of the four members of the *Arabidopsis* *AUX/LAX* family of auxin influx carriers are expressed during embryogenesis. Expression analysis using a translational fusion reporter line (*pAUX1::AUX1-YFP*; Swarup et al., 2004), immuno-localisation (*pAUX1::AUX1-HA*; Swarup et al., 2001) and *in situ* mRNA hybridisation revealed a specific *AUX1* expression pattern in the inner cells at the 32-cell embryo stage and later in the provascular cells (Figs 2A,B, S4A). A similar expression domain was observed for *LAX2*, using *LAX2* transcriptional (*pLAX2::GUS*; Bainbridge et al., 2008) and translational (*pLAX2::LAX2-Venus*; Péret et al., 2012) reporter lines, and immuno-localisation with a specific anti-*LAX2* antibody (Péret et al., 2012). *LAX2* was expressed in provascular cells from the 32-cell stage onwards (Figs 2I,J, S4C,G-I). Additionally, *LAX2* expression was also detected in the hypophysis and the uppermost suspensor cells (Figs 2I,J, S4H,I). The earliest suspensor-specific *LAX2* expression was detected at the 16-cell stage (Figs 2G,H, S4B). In contrast to *AUX1* and *LAX2*, *LAX1* was expressed from the one-cell stage onwards (*pLAX1::GUS*, *pLAX1::LAX1-Venus*; Bainbridge et al., 2008; Péret et al., 2012). *LAX1*

expression was specific to the apical cell and was restricted to the proembryo until the 16-cell stage (Figs 2C,D, S4D). From the 32-cell stage onwards, it gradually became more pronounced in the upper tier (Figs 2E, S4E), consistent with its expression in the upper half of heart stage embryos including the cotyledons (Figs 2F, S4F). No *LAX3* expression could be detected during any stage of embryogenesis (data not shown), consistent with available seed-specific microarray data (Belmonte et al., 2013; Le et al., 2010).

Next, embryo development in the *auxlax Arabidopsis* mutants was investigated. No obvious developmental defects could be observed in the single *aux1*, *lax1*, *lax2* mutants, or in the *aux1lax2* and *lax1lax2* double mutants. Patterning defects in the upper tier as well as in the future root pole could be detected in the *aux1lax1* double mutant, but with a low penetrance ($6/150 = 4\%$, Fig. 3C,M, Table 1). Interestingly, both the frequencies ($77/349 = 22.1\%$), as well as the severity of the defects (Fig. 3) increased significantly in the *aux1lax1lax2* triple mutant embryos, demonstrating a functional redundancy between the members of the AUX/LAX family in mediating embryo development. *aux1lax1lax2* embryos up to the globular stage showed defects in apical-basal axis establishment ($11/125 = 8.8\%$; Fig. 3D) manifested by aberrant division of the uppermost suspensor cells, giving the embryos an elongated shape and an unclear boundary between proembryo and suspensor. The most obvious defect observed from the early heart stage was the vertical symmetric instead of horizontal asymmetric division of the hypophysis ($21/192 = 10.9\%$, Fig. 3E). Older embryos were much more affected and resembled *Brassica* microspore embryos grown in the presence of NOA (Fig. 1). Severe defects affecting both cotyledon and root development could be observed (Fig. 3G-K,M-P). Consistently, these phenotypes were also reflected at the seedling stage, with a penetrance between 15 and 30% (Fig. 3Q,R). In line with the absence of *LAX3* expression, no additional effect could be observed in the *aux1lax1lax2lax3* quadruple mutant compared to the *aux1lax1lax2* triple mutant embryos or in the *lax1lax2lax3* mutant compared to the *lax1lax2 mutant* (Fig. 3, Table 1). Taken together, these observations show that the differentially expressed auxin influx carriers are involved in embryo development.

Auxin influx and efflux as equivalent partners in the auxin flow towards the future root pole

Based on the expression patterns of *AUX1*, *LAX1* and *LAX2* at the globular stage, we speculated that these proteins would contribute to the auxin flow from the future shoot meristem towards the hypophysis or future root pole. To investigate this, the expression of the auxin response reporter *pDR5rev::GFP* (Friml et al., 2003) was examined in the

aux1lax1lax2lax3 background. Whereas wild-type embryos accumulate a strong GFP signal at the hypophysis (Fig. 4A), 29.2% (n = 113) of *aux1lax1lax2lax3* embryos showed a reduced *DR5* reporter activity (Fig. 4B). These results suggest that AUX/LAX-mediated auxin transport contributes to the auxin flow towards the future root pole.

Similar problems in building a strong and focussed auxin signalling maximum in the hypophysis were seen in *pin4* embryos (Friml et al., 2002) and in embryos with a reversed PIN1 polarity (Friml et al., 2004). Therefore we tested the genetic interaction between the *AUX/LAX* and *PIN1/PIN4* genes. The embryonic phenotype was assayed at two different growth locations, firstly at PSB, Ghent, Belgium and secondly at CEITEC/MU, Brno, Czech Republic. We noticed that the phenotype penetrance was lower in Brno where the multiple mutants were analysed. Reasons for these differences and incomplete penetrance are many, ranging from quality of soil, water and light to stability of growth temperature, pest control and watering frequency – especially in view of the susceptibility of auxin production to stress and growth conditions. In Table S1, the phenotype percentages are detailed according to the growth location. The percentages presented in the text below were obtained from plants grown in Brno. In the progeny of *pin1-201/+* plants, 12.5% (n = 353) of the embryos showed defects during cotyledon development, while root pole defects were only occasionally observed (Table S1). In the *aux1lax1lax2* mutant background, 8.1% (n = 459) of the embryos are affected in cotyledon (1.1%) and/or root pole (7%) formation (Table S1). The total frequency of embryo defects in *pin1/+* single, *aux/lax* triple and *pin1/+aux1lax1lax2* quadruple plants was comparable to (12.5%, 8.1%, 14%, n = 353, 459, 129, respectively, Table S1). Interestingly, the majority of the defective *pin1aux1lax1lax2* embryos had a *pin1*-like phenotype (12.4%), i.e. defects in cotyledon formation rather than root pole defects. This suggests that the *pin1* mutation rescues the root pole defects in *aux1lax1lax2* mutant embryos. Similar observations were made using *pin4*. In *pin4-2* single mutant embryos only subtle patterning defects in root and shoot were observed (2.1%, n = 140), including premature divisions of the hypophysis daughter cells or vertical divisions of the uppermost suspensor cells (Fig. 4D). However adding the *pin4-2* mutation to the *aux1lax1lax2* triple mutant rescued the developmental defects from 8.1% (n = 459) in *aux1lax1lax2* to 4.9% (n = 304) in *pin4aux1lax1lax2* (Fig. 4E,F, Table S1). Since PIN4 was shown to partially compensate the loss of PIN1 (Vieten et al., 2005), we also generated the quintuple mutant *pin1-201/+ pin4-2 aux1lax1lax2* and analysed its embryo development. Embryos from *pin1/+pin4aux1lax1lax2* plants displayed 25.8% of defects in cotyledons and only 0.6% in roots (n = 1424, 18 plants, Fig. 4H, Table S1). In the quadruple *pin4aux1lax1lax2* plants, progeny of the same quintuple

mother plant segregating for the *pin1-201* mutation, only 4.1% and 1% (n = 432) of the embryos displayed cotyledons and root defects, respectively. Furthermore, seedlings of *pin1/+pin4aux1lax1lax2* did not have cotyledons and the first true leaves were fused (12.6%, n = 1978, seeds from 15 plants, Fig. 4P). Genotype analysis of 34 of these seedlings indicated that this phenotype was found in homozygous *pin1pin4aux1lax1lax2* quintuple mutants. In addition, aberrant cotyledon development was observed in 5.9% of the *pin1/+pin4aux1lax1lax2* seedlings (Fig. 4O compared to *pin1* in Fig. 4K,L), in a similar proportion as in the *pin4aux1lax1lax2* population (from plants segregating for *pin1-201* mutation) (4.4%, n = 424, seeds from 4 plants, Fig. 4M,N, Table S2). Notably, the root phenotype observed in *aux1lax1lax2* seedlings (4.8%, n = 289, Fig. 4J) was gradually rescued when the *pin* mutations were introduced: 0.6% (n = 349) in *pin4aux1lax1lax2*, 0.5% (n = 554) in *pin1/+aux1lax1lax2* and 0.1% (n = 1978) in *pin1/+pin4aux1lax1lax2* (Table S2).

Taken together, these genetic analyses show that the different *aux/lax* and *pin* mutations have additive effects on cotyledon formation and thus indicate that both auxin influx and efflux carriers play a role in this auxin transport dependent developmental event. However, re-equilibrating auxin transport towards the root pole in *aux/lax* mutants by introducing mutations in efflux carriers rescued the root defects in these embryos, suggesting that a proper auxin signalling for the root pole specification might be restored in the quintuple mutant.

AUX/LAX-mediated auxin import is controlled by the MP-BDL signalling pathway

The defects in the *aux/lax* triple embryos strongly resembled the defects observed in the auxin response mutants *monopteros* (*mp*) and *bodenlos* (*bdl*) (Berleth and Jürgens, 1993; Hamann et al., 1999). *MP* encodes ARF5, an auxin-responsive transcription factor that regulates auxin-dependent gene expression, while *BDL* encodes Aux/IAA12, an auxin-degradable repressor of ARF5 activity. Using qRT-PCR, the expression of the auxin influx carriers was analysed in seedlings expressing an inducible auxin insensitive *bdl* mutant protein (Schlereth et al., 2010). In *pRPS5A::bdl-GR* seedlings, the expression of *AUX1*, *LAX2* and *PIN1* was less strongly induced than in the control (*pRPS5A::BDL-GR*, expressing the *BDL* WT gene) after 1h DEX/NAA co-treatment (Fig. S5A), while the expression of *LAX1* was less affected by this treatment. In line with this, *AUX1* and *LAX2* expression levels were reduced in the *mp* mutant, while *LAX1* expression was reduced, but to a lower extent (Fig. S5A). To confirm the embryonic transcriptional regulation of *AUX1*, *LAX1* and *LAX2* by MP, transcriptional (*LAX1*, *LAX2*) and translational (*AUX1*) reporters were introduced into the *mp* strong mutant allele

background (mp^{B4149}). Whereas *LAX1* expression was not affected (Fig. 5D), *AUX1* and *LAX2* expression were reduced or absent in *mp* embryos (Fig. 5E,F).

Next, the genetic interaction between *MP* and the *AUX/LAX* genes was tested by generating multiple mutants. All mutants were screened for the frequency of *mp*-like defects during embryogenesis, as well as for the percentage of rootless seedlings. In both cases we observed that adding *aux1*, *aux1lax2* or the *aux1lax1lax2* mutations to the incompletely penetrant *mp* allele mp^{S319} both qualitatively and quantitatively enhanced the *mp* phenotype (Fig. 5I,J, Table S3). Based on these results we conclude that *AUX1* and *LAX2* act downstream of the MP-BDL signalling pathway.

Similar transcriptional regulation of the PIN1 auxin efflux carrier by the MP-BDL pathway was demonstrated previously (Weijers et al., 2006). Since we showed that both auxin influx and efflux systems work together during embryo development, we asked to what extent they contribute to MP-mediated embryonic root formation. Both the strong (mp^{B4149}) and the weak (mp^{S319}) *mp* alleles were transformed with $pMP::AUX1$, $pMP::LAX2$ or $pMP::PIN1$ constructs. The *mp/+* T2 segregating lines were screened for the frequency of rootless seedlings (Table S4). None of the constructs affected the percentage of rootless seedlings in the mp^{B4149} background: $25.7 \pm 3.7\%$ in $mp/+ pMP::AUX1$ (28 lines), $25.53 \pm 4.8\%$ in $mp/+ pMP::LAX2$ (31 lines) and $23.2 \pm 5\%$ in $mp/+ pMP::PIN1$ (13 lines) compared to $24.9 \pm 2.6\%$ in $mp^{B4149}/+$. However in the mp^{S319} background, *MP* promoter-driven expression of the auxin transporters enhanced the frequency of rootless seedlings: $9.2 \pm 3.3\%$ in $mp/+ pMP::AUX1$ (33 lines), $13.7 \pm 6.5\%$ in $mp/+ pMP::LAX2$ (29 lines) and $9.58 \pm 4.3\%$ in $mp/+ pMP::PIN1$ (28 lines) compared to $4.6 \pm 1.6\%$ in $mp^{S319}/+$.

Given the cooperative role of auxin influx and efflux carriers, we anticipated that adding one auxin transport component is insufficient to complement the *mp* mutation and moreover disturbs the affected system even more. To test this hypothesis, $mp/+ pMP::AUX1$ and $mp/+ pMP::LAX2$ were crossed to $mp/+ pMP::PIN1$ and F1 progenies were analysed (Tables S5 and S6). F1 progeny of the crosses $mp^{B4149}/+ pMP::AUX1$ x $mp^{B4149}/+ pMP::PIN1$ and $mp^{B4149}/+ pMP::LAX2$ x $mp^{B4149}/+ pMP::PIN1$ produced a similar proportion of rootless seedlings as the control cross (Table S5). When the same experiment was performed in the mp^{S319} background, the same trend was observed in F1 crossed seedlings and individual lines, i.e. an enhancement of the penetrance of mp^{S319} rootless phenotypes (Table S6). We concluded that reconstituting either *AUX1*, or *LAX2* and *PIN1* expression in the provascular expression domain of *mp* embryos is not sufficient to rescue the mp^{B4149} rootless phenotype, and even enhances mp^{S319} defects.

All together these experiments showed that *PINI*, *AUX1* and *LAX2* are under transcriptional control of the MP-BDL auxin-dependent signalling pathway, which is in line with earlier results on *LAX2* (Schlereth et al, 2010). Genetic data suggest that the auxin transport machinery acts downstream of the MP-BDL signalling pathway for root pole formation. However our attempts to rescue *mp* mutations by ectopic expression of auxin transport proteins indicated that restoring proper auxin transport machinery to the root pole is not sufficient to rescue impaired root development in these mutants.

DISCUSSION

While testing the utility of *Brassica napus* microspore embryos as high throughput assay system, we uncovered an unexpected role for auxin influx during early embryo development - unexpected because auxin import during embryogenesis has been studied previously and only a role in mature embryos was reported (Ugartechea-Chirino et al., 2009). More precisely, it was demonstrated that *aux1lax* mutants have a larger radicle root cap along with an aberrant cellular organization of the root tip. By investigating mature embryos only, the earlier role of AUX1/LAX family proteins has probably been overlooked. By performing transcriptional and genetic analyses in *Arabidopsis thaliana* from fertilization onwards we demonstrated that all three auxin importers *AUX1*, *LAX1* and *LAX2* have specific expression patterns during early zygotic embryogenesis and that they act redundantly to specify embryonic root and shoot pole identity and development.

Brassica microspore embryos as a model to study Arabidopsis embryogenesis

Inhibiting auxin influx in *Brassica* embryos using 2-NOA affected cotyledon development. Because 1-NOA was reported to also affect efflux transport (Lanková et al., 2010) and since cellular uptake of NAA is independent of auxin influx carriers (Delbarre et al., 1996), a 1-NOA/NAA co-treatment was performed to dissect the actual effect of 1-NOA on auxin influx. This 1-NOA/NAA co-treatment confirmed the more specific action of 2-NOA and thus indicates that auxin influx in *Brassica* microspore embryos is mainly important for cotyledon development.

Switching from the *Brassica* system to *Arabidopsis* zygotic embryos, we were confronted with some phenotypical differences. While *Brassica* microspore embryos treated with auxin import inhibitors were mainly affected in cotyledon development, *Arabidopsis aux/lax* mutant embryos were mainly affected in root pole formation and to a lesser extent in cotyledon

development. However, given the similarity of the phenotypes and the rescue of the 1-NOA-dependent cotyledon phenotype by NAA treatment, these observations suggest that the defects in cotyledon development are specifically related to disturbed auxin influx machinery. Several reasons for the differences in *Brassica* and *Arabidopsis* phenotypes can be put forward: (i) the different genetic backgrounds; (ii) the differences between pharmacologic and genetic disturbance of auxin import action; (iii) the effect of the sporophytic ovule tissue and the presence of endosperm on zygotic embryo development might differ from the *in vitro* microspore context from which the *Brassica* embryos developed. Despite the phenotypical differences, the *B. napus* microspore embryo system provided an important initial indication for a role for auxin import in *Arabidopsis* embryo development. Moreover, the fact that we observed the expected phenotypic output of treatments with a palette of other compounds affecting various cellular processes shows that the *Brassica napus* system can be used for the pharmacological study of embryo development.

A cooperative role of auxin influx and efflux in embryogenesis

In 16-cell stage *Arabidopsis* embryos the PIN1 auxin transporter switches from an apolar to a polar localization (Friml et al., 2003; Robert et al., 2013; Wabnik et al., 2013). Correspondingly, a directed auxin flow from the future shoot meristem towards the root pole is activated (Friml et al., 2003; Friml et al., 2004; Wabnik et al., 2013). In this paper, we showed that the expression of the auxin influx carrier *AUX1* could be detected at the earliest in the central cells of a 32-cell stage embryo, together with *LAX2* expression from the 32-cell stage onwards. Given their spatial localization pattern and their reported auxin import activity, we hypothesized that *AUX1/LAX*-mediated influx provides auxin to the provasculature for PIN1-mediated directional auxin flow towards the root pole (Fig. 6). Indeed, mutating *AUX1* and *LAX2* together with the functionally redundant *LAX1* importer revealed clear defects in root pole formation and to a lesser extent in cotyledon development. Also, the *DR5* auxin response marker was decreased in the root pole of *aux1lax1lax2lax3* mutant embryos, suggesting a role for auxin influx in shoot pole-to-root pole auxin transport, as previously speculated (Spitzer et al., 2009). Interestingly mutations in the *PIN1* auxin efflux carrier showed opposite developmental defects: mainly cotyledon defects and fewer defects at the root pole. Combining mutations in both auxin efflux and influx carriers using quadruple and quintuple mutants intuitively would suggest stronger defects in both cotyledon and root pole developmental programs. However, whereas the *pin1aux1lax1lax2* quadruple mutant showed

increased penetrance of the cotyledon phenotype, it unexpectedly showed fewer defects in root development compared to the *aux1lax1lax2* triple. An explanation might be found in the tissue-specific expression of the auxin transporters. While *PIN1*, *PIN4*, *AUX1*, *LAX2* are expressed in provascular cells, both *LAX1* and *PIN1* are also expressed in protoderm cells. In the protoderm layer auxin is channeled from the suspensor to the cotyledon tips. Hence, in addition to a disturbed transport in the inner cells, upward auxin transport in the protoderm might also be affected in *pin/aux/lax* quadruple and quintuple mutants. We hypothesize that perturbing auxin transport in the protoderm might result in increased auxin accumulation in the suspensor and decreased auxin delivery to the apical regions, which would explain both the root phenotype rescue in *pin1aux1lax1lax2* embryos and the enhanced frequency of cotyledon defects.

A positive transcriptional feedback of auxin signaling on auxin transport for root development

The MP-BDL-mediated signalling pathway has been repeatedly shown to be crucial for hypophysis specification and hence root pole formation. *MP* expression in the *AUX1/LAX2/PIN1* expression domain drives the expression of both influx and efflux carriers, *AUX1*, *LAX2* and *PIN1*, which are needed to establish the essential auxin response maximum in the root stem cell niche (Fig. 6). The close relationship between auxin transport and auxin signalling is illustrated by the similarities in the *mp* and *aux1lax1lax2* mutant phenotypes. Therefore we investigated the effect of restoring the expression of one or more auxin transport components in the *mp* mutant background. However none of the combinations led to a reduced frequency of *mp*-like defects or a reduction in mutant phenotypes. The most plausible explanation is that reactivation of the auxin transport is not able to activate expression of the MP target genes *TARGET OF MONOPTEROS 5 (TMO5)* and *TMO7*, which were shown to be involved in the MP-controlled root pole development (Schlereth et al., 2010).

Interestingly, although reactivation of one of the auxin components in the *mp* background would intuitively lead to either a small rescue of the *mp* phenotype or to no change in phenotype, the transformed *mp*^{S319} mutants showed an enhanced frequency of the *mp* phenotype, suggesting that the constructs enhanced the *mp*-related defects. We hypothesize that a fully operational and balanced auxin transport in the embryo requires both PIN and AUX/LAX components. This conclusion is consistent with recent findings in *Arabidopsis* root apical tissues (Band et al., 2014). In the *mp* embryos, PIN1-dependent efflux and

AUX1/LAX2-dependent influx machineries are not functional (Figure 5; Weijers et al., 2006). Adding only one component i.e. PIN or AUX/LAX would then disturb the defective system even more. This can be compared with a traffic jam: if an obstruction blocks the road, opening the entrances upstream of the obstruction would only make the traffic jam worse.

Concluding remarks

In this study, we showed the importance of auxin influx machinery for embryo development. In our attempts to uncouple the roles of the AUX/LAX proteins in cotyledon and root developments, we also identified a transcriptional feedback loop in which the MP-BDL auxin signalling pathway regulates *AUX1* and *LAX2* expression in the inner embryonic cells. Interfering with auxin transport from its source in the shoot apical meristem to the future root meristem resulted in aberrant root development. We also identified a cooperative role of auxin influx (*LAX1*) and auxin efflux (*PIN1*) in cotyledon specification. Together these results support the coordinated involvement of both auxin influx and auxin efflux for proper embryo development.

MATERIALS AND METHODS

Plant material and growth conditions

Arabidopsis thaliana seeds were sterilized with chlorine gas, plated on half-strength MS medium (pH 5.7) containing 1% sucrose, 0.01% myo-inositol, 0.05% MES, 0.8% agar, stored for 2 days at 4°C, and grown vertically at 21°C under continuous light. Two weeks after germination, seedlings were transferred to soil and grown at 21°C under long days conditions. The following lines: *aux1-21*, *lax1*, *lax2*, *aux1lax1lax2*, *aux1lax1lax2lax3*, *pin1-201*, *pin4-2*, *pin4-3*, *mp^{B4149}*, *mp^{S319}*, *pDR5rev::GFP*, *pLAX1::LAX1-VENUS*, *pLAX2::LAX2-VENUS*, *pLAX1::GUS*, *pLAX2::GUS*, *pLAX3::GUS*, *pAUX1::AUX1-HA*, *pAUX1::AUX1-YFP*, *pRPS5A::BDL-GR* and *pRPS5A::bdl-GR* were previously described (Bainbridge et al., 2008; Bennett et al., 1996; Cole et al., 2009; Friml et al., 2003; Furutani et al., 2004; Marchant et al., 1999; Péret et al., 2012; Swarup et al., 2004; Weijers et al., 2006).

The following lines were generated by crossing: *aux1lax1*, *aux1lax2*, *lax1lax2*, *lax1lax2lax3*, *pDR5rev::GFP aux1lax1lax2lax3* (generated by crossing *DR5rev::GFP aux1lax1lax2* and *aux1lax1lax2lax3* (Bainbridge et al., 2008)), *pin1-201 aux1lax1lax2*, *pin4-2 aux1lax1lax2*, *pin4-3 aux1lax1lax2*, *pin1-201 pin4-2 aux1lax1lax2*, *mp^{S319} aux1lax1lax2*.

Generation and analysis of ectopic expression of *PIN1*, *AUX1* and *LAX2* in the *mp* background

The *MP* promoter from the *pJet_MP*-promoter vector was cloned in *pDONRP4PIR* using the primers attB4_MP_FOR and attB1R_MP_REV. *PIN1*, *AUX1* and *LAX2* genomic DNA was amplified from *Arabidopsis* seedlings using primers attB1_PIN1_FOR and attB2R_PIN1_REV; attB1_AUX1_FW and attB2R_AUX1_RV; and attB1_LAX2_FW and attB2R_LAX2_RV respectively and Gateway-cloned in the *pDONR221*. Using a multisite gateway reaction *PIN1*, *AUX1* and *LAX2* entry clones were combined with the *MP* promoter into *pH7m24GW*. Heterozygous *mp^{B4149}* and *mp^{S319}* plants were transformed by the floral dip method. T1 transformants were selected for the presence of *mp^{B4149}* and *mp^{S319}* mutations. Hemizygous T2 lines were analysed for *mp*-like phenotype penetrance. A selection of lines were tested for overexpression of the transgenes by qRT-PCR (see below), and grown to obtain T3 homozygous hemizygous *pMP:xx* in *mp^{B4149}/+* and *mp^{S319}/+* backgrounds. Phenotype penetrance was confirmed in T3 homozygous lines. T3 lines were used for crossing *PIN1* to *AUX1* or *LAX2* to simultaneously ectopically express efflux and influx auxin carriers in embryos. F1 seedling phenotypes were scored.

Microspore-induced embryogenesis and chemical treatments

The generation of embryos using double-haploid *Brassica napus* cv Topas DH4079 microspores was performed according to Supena et al (2008). After collecting the microspores, a heat shock of 22 h at 32°C in the dark was applied using a microspore density of 40.000 per ml. Microspores were distributed in 24-well plates (500 µl per well) and incubated at 25°C in dark. Five days after the heat shock, when the microspores had a swollen appearance, compounds (or mock) were added in 500 µl media, bringing the total volume to 1 ml per well. This stage was selected to overcome a putative negative effect of the compounds on the microspore embryo induction program. Microspore embryogenesis was evaluated daily using light microscopy and phenotypes were quantified at 7 days after treatment. Embryos were ranging from globular to torpedo stages. The compounds used in this study were: NAA (α -naphthaleneacetic acid, Duchefa), 2,4-D (2,4-dichlorophenoxyacetic acid, Sigma), PEO-IAA (α -(phenyl ethyl-2-one)-indole-3-acetic acid, a gift from Hayashi's lab), BA (6-Benzylaminopurine, Sigma), NPA (N-1-naphthylphthalamidic acid, Sigma), 1-NOA (1-naphthoxyacetic acid, Sigma), 2-NOA (2-naphthoxyacetic acid, Sigma), brefeldin A (Sigma), wortmannin (Sigma), tyrphostin A23 (Sigma), tyrphostin A51 (Sigma). Stock solutions were diluted in DMSO. Statistical analysis was performed by contingency table X^2 statistical tests.

***In vitro* culture of *Arabidopsis* embryos**

Culture of embryos was carried out as described in (Sauer and Friml, 2008). Culture medium was supplemented with 10 µM 2-NOA in DMSO, or the equivalent amount of DMSO as a solvent control. Seeds originating from siliques 3 and 4, counting from the first dehiscent flower, were cultured for 6 days. Embryos were extracted from the seeds for microscopic analysis. Only embryos from healthy seeds were analysed.

Histological analyses and microscopy

For GUS staining of embryos, embryos were dissected out of the seeds in 90% acetone. For embryos younger than the globular stage, seeds were opened but the embryos were not dissected. After dissection, seeds and embryos were transferred to sieves (BD Falcon, cell strainer 40 µm nylon) and were incubated under vacuum for 10 min in 90% acetone. Subsequently three washing steps were done under vacuum for 10 min each with a 0.5 M phosphate buffer ($\text{Na}_2\text{HPO}_4/\text{NaH}_2\text{PO}_4$ (615/385), pH 7). Sieves were then transferred to GUS staining solution (X-Glu (1 mM) dissolved in DMFO (0.5% v/v); Triton X-100 (0.5% v/v);

EDTA (1 mM); $K_3Fe(CN)_6$ (0.5 mM); $K_4Fe(CN)_6$ (0.5 mM); phosphate buffer (0.5 M); pH 7) and incubated for 1 h under vacuum. After vacuum infiltration, samples were incubated at 37 °C. The staining reaction was stopped by two washes with 0.5 M phosphate buffer under vacuum for 10 min each. Embryos were transferred to slides, mounted with 10% glycerol and analysed with a DIC fluorescence microscope (Olympus).

Immunofluorescence analyses of *Arabidopsis* embryos were performed as previously described (Sauer et al., 2006b) using mouse anti-HA (1/600, Life Technologies), rabbit anti-LAX2 (1/200; Péret et al., 2012) mouse anti-GFP (1/600, Sigma), Cy3-conjugated goat anti-mouse (1/600, Sigma) and anti-rabbit (1/600, Sigma), and Alexa488-conjugated goat anti-mouse (1/600, Life Technology). Nuclei were stained with DAPI (1 mg/L in water, Sigma).

For GFP visualization, embryos were fixed in 4% PFA in PBS buffer (pH 7.4) and prepared on slides as described (Sauer et al., 2006b). Embryos were rehydrated in water, and when indicated stained for 2 h in SCRI Renaissance 2200 (2% in 4% DMSO/water solution, Renaissance Chemicals), washed twice in water and mounted with an anti-fading solution.

For *Arabidopsis in vitro*-cultured embryos, GFP was visualized after dissection from the seed in a 5% glycerol/water solution.

For embryo phenotyping, embryos were cleared at the indicated stages in a chloral hydrate solution (chloral hydrate/water/glycerol, 8/3/1, w/v/v).

Whole-mount *in situ* hybridization of embryos was carried out as previously described (Hejátko et al., 2005) using a full-length *AUX1* RNA probe (see Table S7 for primer sequences). Embryos were analysed by clearing seeds in chloral hydrate.

Confocal imaging was performed on Zeiss Exciter 5, Zeiss 710 and Zeiss 780 confocal laser scanning microscopes using 405 nm (DAPI, Renaissance), 488 nm (YFP, GFP, Alexa488) or/and 543 nm (Cy3) excitation filters with 420-480 nm band pass (DAPI, Renaissance), 505-530 nm band pass (GFP, YFP, Alexa488) and 560 nm long pass (Cy3) emission filters. Acquisition with multiple channels was performed by sequential scanning. Microscopy observations were performed on a DIC fluorescence microscope (Olympus). Images were processed in Adobe Photoshop CS and assembled in Adobe Illustrator CS.

RNA extraction, cDNA synthesis and qRT-PCR analysis

Experiment was set up according to Schlereth et al (2010). *pRPS5A::BDL-GR*, *pRPS5A::bdl-GR*, *mp^{B4149}* and Col seedlings were grown for 5 days, were treated in liquid medium with 10 μM Dexamethasone (DEX, Santa Cruz) for 1 h, then co-treated with 10 μM NAA and 10 μM DEX for 1 h, 2 h and 4 h. Presented data are from 1h co-treatment. For RNA extraction, whole

seedlings were ground in liquid nitrogen and total RNA was isolated with Trizol (Invitrogen) according to the manufacturer's instructions. Poly(dT) cDNA was prepared from 2 µg total RNA with Superscript III reverse transcriptase (Invitrogen) and quantified on an LightCycler 480 apparatus (Roche Diagnostics) with the SYBR Green I Master kit (Roche Diagnostics) according to the manufacturer's instructions. All individual reactions were carried out in triplicate. Data were analysed with qBase (Hellemans et al., 2007). Expression levels of *AUX1*, *LAX1*, *LAX2*, *LAX3* and *PIN1* were normalized to those of *EEF1α4* and *CDKA*, which showed no clear systematic changes in Ct values. Data from *BDL-GR* were compared with *bdl-GR* and from *mp* with Col.

Acknowledgements

We thank Cris Kuhlemeier, Ken-Ichiro Hayashi for providing material, Agnieszka Bielach for support with statistical analysis, N. Smet, and the PSB transformation facility for technical assistance. W.G. is a post-doctoral fellow of the Research Foundation Flanders. H.S.R is supported by Employment of Best Young Scientists for International Cooperation Empowerment (CZ.1.07/2.3.00/ 30.0037), co-financed by the European Social Fund and the state budget of the Czech Republic. Mi.S. was funded by the Ramón y Cajal program. This work was supported by the European Research Council (project ERC-2011-StG-20101109-PSDP), project “CEITEC - Central European Institute of Technology” (CZ.1.05/1.1.00/02.0068), the European Social Fund (CZ.1.07/2.3.00/20.0043), and the Czech Science Foundation GACR (GA13-40637S) to J.F. We acknowledge funding from the BBSRC (Biological and Biotechnological Science Research Council) and EPSRC (Engineering Physics Science Research Council) to R.S. and M.B.

Author Contributions

W.G., H.S.R. and J.F. designed the project. W.G. performed the *Brassica* microspore embryo related work, cloning and generation of the MP complementation lines. W.G. and H.S.R. performed the expression analysis of the reporter lines. Mi.S. performed the *Arabidopsis* ovule culture and treatments. W.G., H.S.R., B.C. and R.S. generated mutant lines. W.G., H.S.R. performed the genetic analysis and analyzed the data. Me.S., K.B., R.S., D.W. and M.B. provided unpublished material and methods. W.G. and H.S.R. prepared the manuscript. Mi.S. M.B., D.W., Me.S., K.B. and J.F. edited the manuscript prior to submission.

References

- Bainbridge, K., Guyomarc'h, S., Bayer, E. E., Swarup, R., Bennett, M. J., Mandel, T. T. and Kuhlemeier, C.** (2008). Auxin influx carriers stabilize phyllotactic patterning. *Genes Dev.* **22**, 810–823.
- Band, L. R., Wells, D. M., Fozard, J. A., Ghetiu, T., French, A. P., Pound, M. P., Wilson, M. H., Yu, L., Li, W., Hijazi, H. I., et al.** (2014). Systems analysis of auxin transport in the Arabidopsis root apex. *Plant Cell* **26**, 862–875.
- Belmonte, M. F., Kirkbride, R. C., Stone, S. L., Pelletier, J. M., Bui, A. Q., Yeung, E. C., Hashimoto, M., Fei, J., Harada, C. M., Munoz, M. D., et al.** (2013). Comprehensive developmental profiles of gene activity in regions and subregions of the Arabidopsis seed. *Proc Natl Acad Sci USA* **110**, E435–44.
- Bennett, M. J., Marchant, A., Green, H. G., May, S. T., Ward, S. P., Millner, P. A., Walker, A. R., Schulz, B. and Feldmann, K. A.** (1996). Arabidopsis AUX1 gene: a permease-like regulator of root gravitropism. *Science* **273**, 948–950.
- Berleth, T. and Jürgens, G.** (1993). The role of the monopteros gene in organising the basal body region of the Arabidopsis embryo. *Development* **118**, 575–587.
- Cole, M., Chandler, J., Weijers, D., Jacobs, B., Comelli, P. and Werr, W.** (2009). DORNROSCHEN is a direct target of the auxin response factor MONOPTEROS in the Arabidopsis embryo. *Development* **136**, 1643–1651.
- Delbarre, A., Muller, P., Imhoff, V. and Guern, J.** (1996). Comparison of mechanisms controlling uptake and accumulation of 2,4-dichlorophenoxy acetic acid, naphthalene-1-acetic acid, and indole-3-acetic acid in suspension-cultured tobacco cells. *Planta* **198**, 532–541.
- Friml, J., Benková, E., Blilou, I., Wiśniewska, J., Hamann, T., Ljung, K., Woody, S., Sandberg, G., Scheres, B., Jürgens, G., et al.** (2002). AtPIN4 mediates sink-driven auxin gradients and root patterning in Arabidopsis. *Cell* **108**, 661–673.
- Friml, J., Vieten, A., Sauer, M., Weijers, D., Schwarz, H., Hamann, T., Offringa, R. and Jürgens, G.** (2003). Efflux-dependent auxin gradients establish the apical-basal axis of Arabidopsis. *Nature* **426**, 147–153.
- Friml, J., Yang, X., Michniewicz, M., Weijers, D., Quint, A., Tietz, O., Benjamins, R., Ouwerkerk, P. B. F., Ljung, K., Sandberg, G., et al.** (2004). A PINOID-dependent binary switch in apical-basal PIN polar targeting directs auxin efflux. *Science* **306**, 862–865.
- Furutani, M., Vernoux, T., Traas, J., Kato, T., Tasaka, M. and Aida, M.** (2004). PINFORMED1 and PINOID regulate boundary formation and cotyledon development in Arabidopsis embryogenesis. *Development* **131**, 5021–5030.
- Geldner, N., Friml, J., Stierhof, Y.-D., Jürgens, G. and Palme, K.** (2001). Auxin transport inhibitors block PIN1 cycling and vesicle trafficking. *Nature* **413**, 425–428.

- Hamann, T., Mayer, U. and Jürgens, G.** (1999). The auxin-insensitive bodenlos mutation affects primary root formation and apical-basal patterning in the Arabidopsis embryo. *Development* **126**, 1387–1395.
- Hayashi, K.-I. K., Tan, X., Zheng, N., Hatate, T., Kimura, Y., Kepinski, S. and Nozaki, H.** (2008). Small-molecule agonists and antagonists of F-box protein-substrate interactions in auxin perception and signaling. *Proc Natl Acad Sci U S A* **105**, 5632–5637.
- Hejátko, J., Blilou, I., Brewer, P. B., Friml, J., Scheres, B. and Benková, E.** (2005). In situ hybridization technique for mRNA detection in whole mount Arabidopsis samples. *Nat. Protocols* **1**, 1939–1946.
- Hellemans, J., Mortier, G., De Paepe, A., Speleman, F. and Vandesompele, J.** (2007). qBase relative quantification framework and software for management and automated analysis of real-time quantitative PCR data. *Genome Biol* **8**, R19.
- Jones, A. R., Kramer, E. M., Knox, K. K., Swarup, R., Bennett, M. J., Lazarus, C. M., Leyser, O. O. and Grierson, C. S.** (2009). Auxin transport through non-hair cells sustains root-hair development. *Nat Cell Biol* **11**, 78–84.
- Joosen, R., Cordewener, J., Supena, E. D. J., Vorst, O., Lammers, M., Maliepaard, C., Zeilmaker, T., Miki, B., America, T., Custers, J., et al.** (2007). Combined transcriptome and proteome analysis identifies pathways and markers associated with the establishment of rapeseed microspore-derived embryo development. *Plant Physiol* **144**, 155–172.
- Kierzkowski, D., Lenhard, M. M., Smith, R. and Kuhlemeier, C.** (2013). Interaction between Meristem Tissue Layers Controls Phyllotaxis. *Dev. Cell* **26**, 616–628.
- Lanková, M., Smith, R. S., Pesek, B., Kubes, M., Zazimalová, E., Petrásek, J. and Hoyerová, K.** (2010). Auxin influx inhibitors 1-NOA, 2-NOA, and CHPAA interfere with membrane dynamics in tobacco cells. *J Exp Bot.* **61**, 3589–3598.
- Le, B. H., Cheng, C., Bui, A. Q., Wagmaister, J. A., Henry, K. F., Pelletier, J., Kwong, L. W., Belmonte, M., Kirkbride, R., Horvath, S., et al.** (2010). Global analysis of gene activity during Arabidopsis seed development and identification of seed-specific transcription factors. *Proc Natl Acad Sci USA* **107**, 8063–8070.
- Ljung, K., Hull, A. K., Celenza, J. L., Yamada, M., Estelle, M., Normanly, J. and Sandberg, G.** (2005). Sites and regulation of auxin biosynthesis in Arabidopsis roots. *Plant Cell* **17**, 1090–1104.
- Marchant, A., Kargul, J., May, S. T., Muller, P., Delbarre, A., Perrot-Rechenmann, C. and Bennett, M. J.** (1999). AUX1 regulates root gravitropism in Arabidopsis by facilitating auxin uptake within root apical tissues. *EMBO J* **18**, 2066–2073.
- Marhavy, P., Bielach, A. A., Abas, L., Abuzeineh, A., Duclercq, J., Tanaka, H., Pařezová, M., Petrásek, J., Friml, J., Kleine-Vehn, J., et al.** (2011). Cytokinin Modulates Endocytic Trafficking of PIN1 Auxin Efflux Carrier to Control Plant Organogenesis. *Dev. Cell* **21**, 796–804.
- Marhavy, P., Duclercq, J., Weller, B., Feraru, E., Bielach, A. A., Offringa, R., Friml, J.,**

- Schwechheimer, C. C., Murphy, A. S. and Benková, E.** (2014). Cytokinin Controls Polarity of PIN1-Dependent Auxin Transport during Lateral Root Organogenesis. *Curr. Biol.* **24**, 1031–1037.
- Parry, G., Delbarre, A., Marchant, A., Swarup, R., Napier, R., Perrot-Rechenmann, C. and Bennett, M. J.** (2001). Novel auxin transport inhibitors phenocopy the auxin influx carrier mutation *aux1*. *Plant J* **25**, 399–406.
- Petersson, S. V., Johansson, A. I., Kowalczyk, M., Makoveychuk, A., Wang, J. Y., Moritz, T., Grebe, M., Benfey, P. N., Sandberg, G. and Ljung, K.** (2009). An auxin gradient and maximum in the Arabidopsis root apex shown by high-resolution cell-specific analysis of IAA distribution and synthesis. *Plant Cell* **21**, 1659–1668.
- Petrásek, J. and Friml, J.** (2009). Auxin transport routes in plant development. *Development* **136**, 2675–2688.
- Péret, B., Swarup, K., Ferguson, A., Seth, M., Yang, Y., Dhondt, S., James, N., Casimiro, I., Perry, P. P., Syed, A., et al.** (2012). AUX/LAX Genes Encode a Family of Auxin Influx Transporters That Perform Distinct Functions during Arabidopsis Development. *Plant Cell* **24**, 2874–2885.
- Rademacher, E. H., Lokerse, A. S., Schlereth, A., Llavata Peris, C., Bayer, M., Kientz, M., Freire Rios, A., Borst, J. W., Lukowitz, W., Jürgens, G., et al.** (2012). Different Auxin Response Machineries Control Distinct Cell Fates in the Early Plant Embryo. *Dev. Cell* **22**, 211–222.
- Robert, H. S., Grones, P., Stepanova, A. N., Robles, L. M., Lokerse, A. S., Alonso, J. M., Weijers, D. and Friml, J.** (2013). Local auxin sources orient the apical-basal axis in Arabidopsis embryos. *Curr. Biol.* **23**, 2506–2512.
- Růžicka, K., Simásková, M., Duclercq, J., Petrásek, J., Zazímalová, E., Simon, S., Friml, J., Van Montagu, M. C. E. and Benková, E.** (2009). Cytokinin regulates root meristem activity via modulation of the polar auxin transport. *Proc Natl Acad Sci USA* **106**, 4284–4289.
- Sauer, M., Balla, J., Luschign, C., Wisniewska, J., Reinöhl, V., Friml, J. and Benková, E.** (2006a). Canalization of auxin flow by Aux/IAA-ARF-dependent feedback regulation of PIN polarity. *Genes Dev.* **20**, 2902–2911.
- Sauer, M., Paciorek, T., Benková, E. and Friml, J.** (2006b). Immunocytochemical techniques for whole-mount in situ protein localization in plants. *Nat. Protocols* **1**, 98–103.
- Sauer, M and Friml, J** (2008). In Vitro Culture of Arabidopsis Embryos. *Methods Mol. Biol.* **427**, 71–76.
- Schlereth, A., Möller, B., Liu, W., Kientz, M., Flipse, J., Rademacher, E. H., Schmid, M., Jürgens, G. and Weijers, D.** (2010). MONOPTEROS controls embryonic root initiation by regulating a mobile transcription factor. *Nature* **464**, 913–913.
- Spitzer, C., Reyes, F. C., Buono, R., Sliwinski, M. K., Haas, T. J. and Otegui, M. S.** (2009). The ESCRT-related CHMP1A and B proteins mediate multivesicular body

sorting of auxin carriers in Arabidopsis and are required for plant development. *Plant Cell* **21**, 749–766.

- Supena, E. D. J., Winarto, B., Riksen, T., Dubas, E., Van Lammeren, A., Offringa, R., Boutilier, K. and Custers, J.** (2008). Regeneration of zygotic-like microspore-derived embryos suggests an important role for the suspensor in early embryo patterning. *J Exp Bot.* **59**, 803–814.
- Swarup, K., Benková, E., Swarup, R., Casimiro, I., Péret, B., Yang, Y., Parry, G., Nielsen, E., De Smet, I., Vanneste, S., et al.** (2008). The auxin influx carrier LAX3 promotes lateral root emergence. *Nat Cell Biol* **10**, 946–954.
- Swarup, R., Friml, J., Marchant, A., Ljung, K., Sandberg, G., Palme, K. and Bennett, M. J.** (2001). Localization of the auxin permease AUX1 suggests two functionally distinct hormone transport pathways operate in the Arabidopsis root apex. *Genes Dev.* **15**, 2648–2653.
- Swarup, R., Kargul, J. J., Marchant, A. A., Zadik, D. D., Rahman, A. A., Mills, R. R., Yemm, A. A., May, S. S., Williams, L. L., Millner, P. P., et al.** (2004). Structure-function analysis of the presumptive Arabidopsis auxin permease AUX1. *Plant Cell* **16**, 3069–3083.
- Ugartechea-Chirino, Y., Swarup, R., Swarup, K., Péret, B., Whitworth, M., Bennett, M. J. and Bougourd, S.** (2009). The AUX1 LAX family of auxin influx carriers is required for the establishment of embryonic root cell organization in Arabidopsis thaliana. *Annals of Botany*.
- Ulmasov, T., Murfett, J., Hagen, G. and Guilfoyle, T. J.** (1997). Aux/IAA proteins repress expression of reporter genes containing natural and highly active synthetic auxin response elements. *Plant Cell* **9**, 1963–1971.
- Vieten, A., Vanneste, S., Wiśniewska, J., Benková, E., Benjamins, R., Beeckman, T., Luschnig, C. and Friml, J.** (2005). Functional redundancy of PIN proteins is accompanied by auxin-dependent cross-regulation of PIN expression. *Development* **132**, 4521–4531.
- Wabnik, K., Robert, H. S., Smith, R. S. and Friml, J.** (2013). Modeling framework for the establishment of the apical-basal embryonic axis in plants. *Curr. Biol.* **23**, 2513–2518.
- Weijers, D., Schlereth, A., Ehrismann, J. S., Schwank, G., Kientz, M. and Jürgens, G.** (2006). Auxin triggers transient local signaling for cell specification in Arabidopsis embryogenesis. *Dev. Cell* **10**, 265–270.
- Yoshida, S., de Reuille, P. B., Lane, B., Bassel, G. W., Prusinkiewicz, P. P., Smith, R. S. and Weijers, D.** (2014). Genetic control of plant development by overriding a geometric division rule. *Dev. Cell* **29**, 75–87.

Figures legends

Figure 1. Auxin influx is required for proper embryogenesis

Brassica napus microspore embryos (A-C) treated with 1-NOA (B, C) displayed fused cotyledons (B) and aberrant root development (C) phenotypes. *Arabidopsis thaliana* zygotic embryos of *aux1lax1lax2* triple mutant (E, F) at heart stage phenotypes resemble *B. napus* microspore embryos cultured in the presence of 1-NOA. WT (D) is presented. *Arabidopsis thaliana* zygotic embryos cultured in the presence of 2-NOA (H, I, K, L) displayed fused cotyledons (H, K) and aberrant root development (I, L) phenotypes. The results of the DMSO treated controls are shown in (A, G, J). (G-I) show light and (J-L) fluorescence images of the *pDR5rev::GFP* signal in the same embryos. Scale bars represent 50 μm (A-C) and 20 μm (D-L).

Figure 2. AUX1, LAX1 and LAX2 are expressed during embryogenesis.

AUX1 (A, B), *LAX1* (C-F) and *LAX2* (G-J) are expressed during embryo development. *AUX1* is expressed from the 32-cell stage in the inner cells as detected by RNA *in situ* hybridization (A, purple signal) and after immuno-localization of the YFP tag using anti-GFP antibodies in *pAUX1::AUX1-YFP* embryos (B, green signal, nuclei are stained in blue). *LAX1* is expressed in the proembryo from the 1-cell stage (C) till the early globular stage (D). Its expression is then progressively enhanced in the apical embryo tier at the late globular stage (E) and restricted to the cotyledon tips at the heart stage (F, late heart), as detected in *pLAX1::GUS* embryos. *LAX2* is first expressed in suspensor cells at the globular stage (H). No expression is detected before this stage, as illustrated in an 8-cell embryo (G). *LAX2* expression shifts to the provascular cells from late globular/transition stage (I) as detected in *pLAX2::GUS*. A late heart stage is shown in (J). Scale bars represent 20 μm .

Figure 3. aux1, lax1 and lax2 mutations affect both cotyledon and root formation

(A-P) Embryo development (A, D, early globular; B, C, E, late globular; F-J, heart; K-P, torpedo stages) is defective in different combinations of *auxlax* mutations. The genotype of the presented embryo is indicated in each panel. These phenotypes are observed in each genotype at various penetrances. WT embryos are shown for comparison (A, B, F, L) to *aux1lax1* (C, M), *aux1lax1lax2* (D, G, H, K, N) and *aux1lax1lax2lax3* (E, I, J, O, P). (Q, R) Examples of *aux1lax1lax2* seedling phenotypes: a stubby hypocotyl (R) and monocotyledon with an underdeveloped root (Q). Scale bars represent 10 μm (A-E), 20 μm (F-J) and 50 μm

(K-P). White arrowheads (C, E, G, M) and line (D) indicate deviation in the WT development.

Figure 4. *pin1* and *pin4* mutations rescued *auxlax* root phenotypes

(A, B) *pDR5rev::GFP* auxin reporter expression is reduced in *aux1lax1lax2lax3* embryos (B) compared to WT (A). (C-H) Embryo phenotype observed in *pin4* (D, arrowhead points to cell division in the uppermost suspensor cell), *pin4aux1lax1lax2* (E, F) and in *pin1/+ pin4aux1lax1lax2* (H). WT embryos are shown for comparison (C, G). (I-P) After germination, seedlings of *aux1lax1lax2* (J), *pin1-201* (K, L), *pin4aux1lax1lax2* (M, N), *pin1/+ pin4aux1lax1lax2* (O), *pin1pin4aux1lax1lax2* (P) are affected in cotyledon and root development. A WT seedling is shown for comparison (I). Scale bars represent 20 μm . White arrowheads (B, D, E) and line (F) indicate deviation in the WT development.

Figure 5. MP/BDL transcriptional pathway regulates *AUX1* and *LAX2* expression

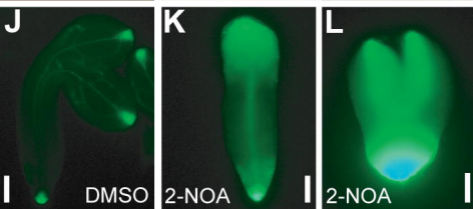
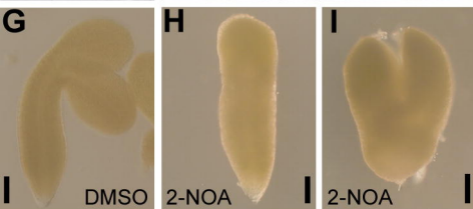
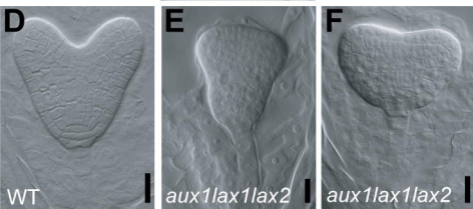
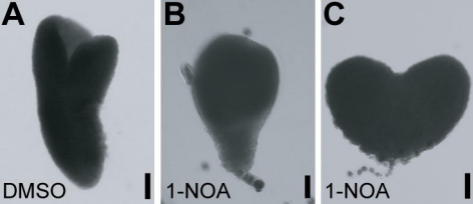
(A-F) *LAX2* (B, E) and *AUX1* (C, F), but not *LAX1* (A, D), expression is absent in *mp*^{B4149} embryos (D-F), compared to WT embryos (A-C). (G-J) Seedlings phenotypes of *mp*^{S319} (G), *aux1lax1lax2* (H) and *mp*^{S319}*aux1lax1lax2* (I, J). Scale bars represent 20 μm .

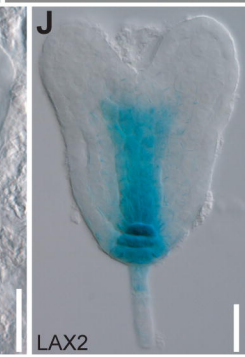
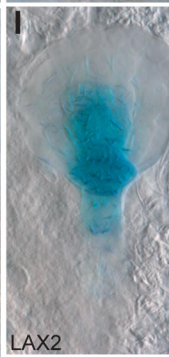
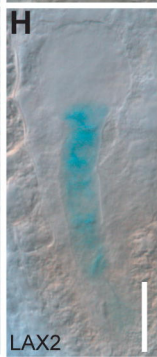
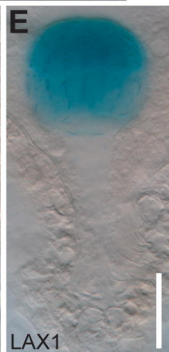
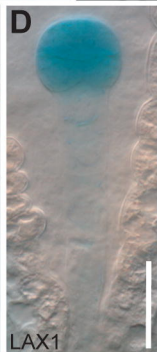
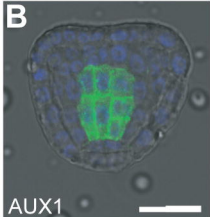
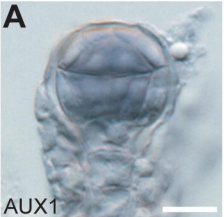
Figure 6. A model for a balanced and regulated auxin transport during embryo development

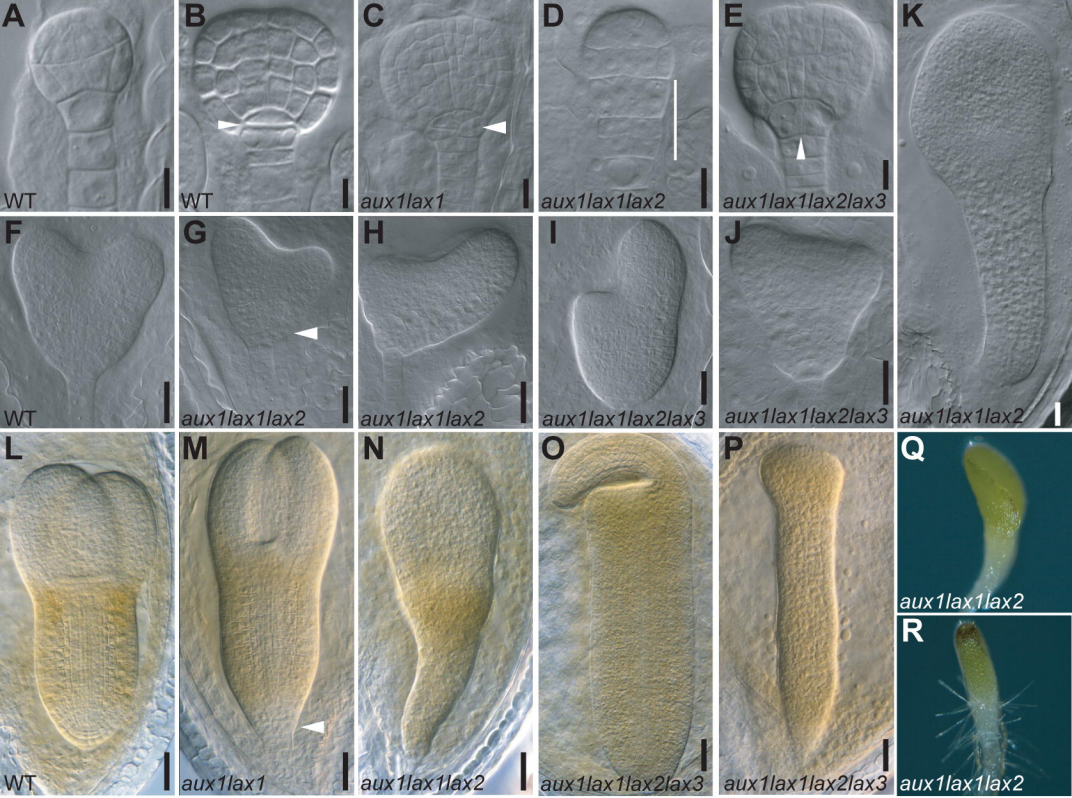
Local auxin production occurs in the two opposite poles of the embryo, in the suspensor and the shoot apical meristem (purple). Auxin is transported by PIN1 (dark blue arrows) and LAX1 (yellow line) from the suspensor to the tips of the cotyledons via the protoderm. Auxin is transported by efflux (PIN1, dark blue arrows, and PIN4, light blue arrows) and influx (AUX1 and LAX2, orange) transporters from the shoot apical meristem to the root meristem, where it accumulates (green) and triggers auxin signalling. From the root meristem, auxin is transported away from the embryo by PIN7 (purple arrows). Transcriptional feedback involving MONOPTEROS (MP, light green dashed arrow) regulates expression of *PIN1*, *AUX1* and *LAX2* in the inner embryonic cells.

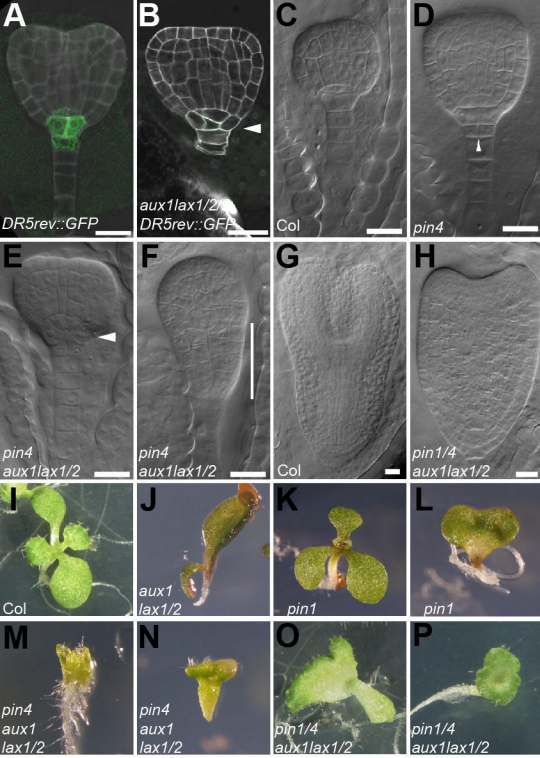
Table 1. Summary of *aux lax* mutant combinations with embryo phenotypes

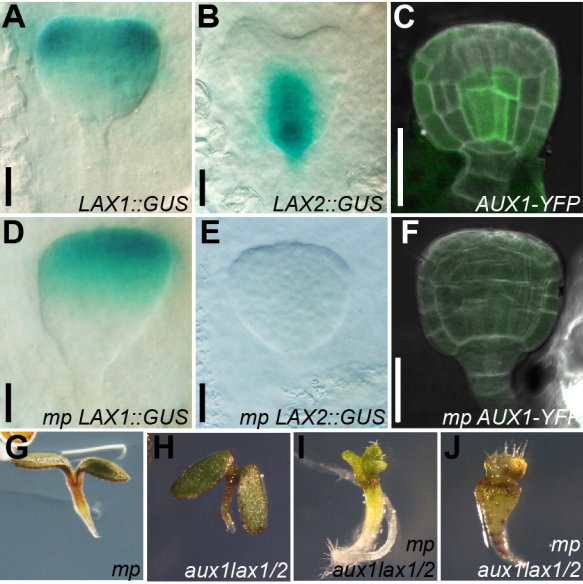
Lines	Phenotypes	n	% embryo defects from late globular stage on	References for the line
<i>aux1</i>	none	465	0	Bennett, 1996
<i>lax1</i>	none	233	0	Bainbridge, 2008
<i>lax2</i>	none	165	0	Bainbridge, 2008
<i>aux1lax1</i>	Low penetrance for shoot and root specification problem	150	4	this study
<i>aux1lax2</i>	none	360	0	this study
<i>lax1lax2</i>	none	187	0	this study
<i>lax1lax2lax3</i>	none	205	0	this study
<i>aux1lax1lax2</i>	Enhanced penetrance and strength of <i>aux1lax1</i> phenotypes	349	22.1	Bainbridge, 2008
<i>aux1lax1lax2lax3</i>	No additive effects to <i>aux1lax1lax2</i>	208	23.1	Bainbridge, 2008

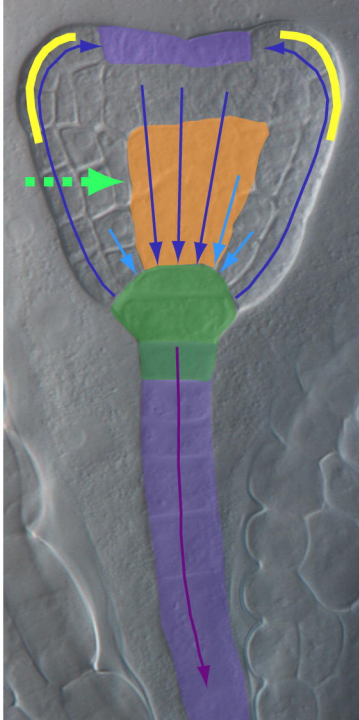













 Auxin Biosynthesis

 Auxin Signalling

 MP/BDL dependent auxin signalling feedback loop

Auxin Transport machinery

 PIN1

 PIN4

 PIN7

 LAX1

 AUX1, LAX2